PERGAMON

Carbon 40 (2002) 1883–1890

CARBON

Quantification and application of skew of breakthrough curves for gases and vapors eluting from activated carbon beds

G.O. Wood*

Los Alamos National Laboratory, Mail Stop K-486, Los Alamos, NM 87545, USA

Received 6 June 2001; accepted 25 November 2001

Abstract

Vapor and gas breakthrough curves for packed activated carbon beds are often assumed to be symmetrical, when they are actually more often skewed. This skew explains why adsorption rate coefficients calculated at differing breakthrough fractions may not agree. Three extensive databases of breakthrough curves were analyzed to quantify this skew and the effects of relative humidity (preconditioning and use) on it. Skew results for varieties of chemicals and carbons agreed well and were combined to get a quadratic expression for a defined skew parameter. This expression was combined with a previous observation of the effect of breakthrough fraction on calculated rate coefficient. The combination allows estimation of an adsorption rate coefficient at a desired breakthrough fraction from a rate coefficient known (experimentally or by calculation) at another breakthrough fraction. A sample calculation is given.

Keywords: A. Activated carbon; C. Adsorption; D. Adsorption properties

1. Introduction

Packed beds of granules of activated carbon are widely used for purifying air for respiratory protection, environmental protection, and chemical processes such as solvent recovery. Process designs and use procedures require knowing when adsorption beds are depleted and need changing. Predictive service life models must incorporate vapor properties, carbon properties, bed parameters, use conditions, equilibrium adsorption capacities, and adsorption rates. The impetus for this study of breakthrough curves was an effort to update and refine the prediction of adsorption rate coefficients for use in one such model [1].

Lodewyckx and Vansant [2] have developed a new empirical correlation for organic vapor/activated carbon adsorption rate coefficients. They used adsorption capacities calculated by the Wood [3] correlation combined with measured 0.1% (of challenge concentration) breakthrough times for a variety of vapors and carbons. However, as Wood and Stampfer [4] have shown, rate coefficients can differ at different breakthrough fractions. This difference is due to unsymmetrical (skewed), nonideal breakthrough curves often observed. Only by quantifying this skew can we use a rate coefficient calculated at one breakthrough fraction (e.g., 0.1%) to get the rate coefficient we need at another breakthrough fraction (e.g., 1%).

2. Theoretical background

The useful service life of an activated carbon adsorbent bed can be defined as a point on a breakthrough curve of the vapor of concern. A breakthrough curve (Fig. 1) is a plot of vapor (or gas) concentration (or relative concentration) measured in the flowing carrier gas (usually air) leaving a fixed packed bed of adsorbent granules as a function of time. When the entering vapor concentration and airflow rate are kept constant and physical adsorption is the removal mechanism, the breakthrough curve typically has the S-shape [5] shown in Fig. 1.

A breakthrough curve is defined by three characteristics: geometric midpoint (stoichiometric time and corresponding relative concentration), steepness, and shape. The midpoint is determined by the airflow rate, the concentration, and the capacity of the adsorbent bed for the vapor at the

*Tel.: +1-505-667-9824; fax: +1-505-665-2192.
E-mail address: gerry@lanl.gov (G.O. Wood).

0008-6223/02/$ – see front matter
PII: S0008-6223(02)00031-3

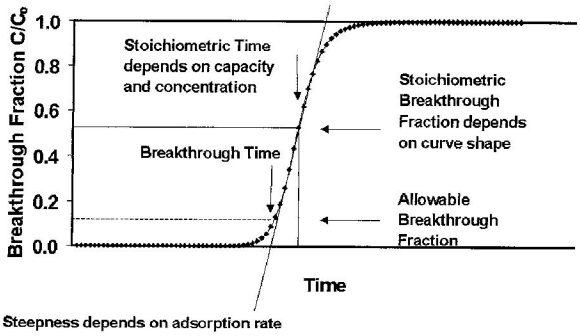

Fig. 1. Characteristics of a typical adsorption breakthrough curve.

relevant vapor concentration and temperature. The steepness of a breakthrough curve is related to the rate (speed) at which the vapor is removed from the air as it flows through the bed. In the simplest case, steepness is described by an overall mass-transfer (adsorption) rate coefficient, which is larger for larger adsorption rates. If this rate coefficient is constant throughout the breakthrough process, the shape of the breakthrough curve will be symmetrical. However, it has often been observed [4,6–8] that breakthrough curves are skewed (asymmetrical), usually steeper at the beginning of breakthrough than at the end.

Such skewed breakthrough curves, steeper at the beginning of breakthrough than predicted by ideal models, can be attributed to heterogeneity of the activated carbon and its adsorption sites in micropores. Vapors at the forefront of the adsorption wave, as it moves through a packed bed, contact and occupy the most active (by rate and capacity) adsorption sites, leaving the less active ones for subsequently arriving vapors.

Bohart and Adams [9] first developed an equation describing the ideal, symmetrical breakthrough curve. They assumed mass balance and constant adsorption kinetics, first order in vapor concentration and first order in concentration of remaining adsorption sites. With the exception of very small values of capacity and time, their equation can be rearranged to express breakthrough time t_b (min) for a breakthrough concentration of C as

$$t_b = \frac{a_o z}{60 v_L C_o} - \frac{1}{k C_o} \ln\left(\frac{C_o - C}{C}\right), \quad (1)$$

where C_o (g/cm^3) is the entering (challenge) concentration, a_o is the volumetric capacity (g/cm^3) of the sorbent for the vapor, z is the bed depth (cm), and v_L is the linear airflow velocity (cm/s). In this case the rate coefficient k has units of cm^3/(g-min). This equation predicts that breakthrough time is on a curve centered at the first (capacity) term on the right-hand side of Eq. (1) and spread symmetrically according to the logarithmic term and to an extent determined by the (constant) first-order adsorption rate coefficient, k. So many others (see Refs. [10–12]) have also derived this equation that it may be best to call it according to a generic designation, the Reaction Kinetic Equation [12].

Mecklenburg [13] also used mass conservation to derive an equation with a capacity term minus a term that includes an undefined 'dead layer' or 'critical bed depth', I:

$$t_b = \frac{a_o A}{C_o Q}[z - I], \quad (2)$$

where Q is the volumetric airflow rate (cm^3/min) and A is the cross-section (cm^2) of the adsorbent bed. Klotz [14] combined the Mecklenburg approach with an expression derived by Gamson et al. [15] for the critical bed depth, I_t, to get a breakthrough time expression, which is sometimes called the Mecklenburg Equation [5]:

$$t_b = \frac{a_o A}{C_o Q}\left[z - \frac{1}{a} Re^{0.41} Sc^{0.67} \ln\left(\frac{C_o}{C}\right)\right]. \quad (3)$$

(Definitions of parameters a, Re, and Sc in this equation are not important for the immediate discussion; they can be found in Ref. [15].) Note that the logarithmic term is different from that in Eq. (1). Klotz replaced $(C_o - C)$ with C_o, by assuming that the C_o/C is very large, i.e., that the breakthrough fraction is very small. This unnecessary assumption was repeated by others [16,17] and incorporated into the best-known breakthrough equation, often called the Modified Wheeler Equation [17] or Wheeler–Jonas Equation [2]:

$$t_b = \frac{W_e W}{C_o Q} - \frac{W_e \rho_B}{k_v C_o} \ln\left(\frac{C_o}{C}\right), \quad (4)$$

where W_e is the gravimetric (g/g carbon) capacity, W is the weight (g) of carbon, and ρ_B is the packed density (g/cm^3) of the carbon bed. The substitution of $\ln(C_o/C)$ for $\ln[(C_o - C)/C]$ makes less than 1% difference in the second (kinetic) term of Eq. (4) for breakthrough fractions C/C_o less than 0.032. However, it does change the shape of the breakthrough curve from S-shaped to J-shaped, approaching infinity instead of a maximum value at long times (Fig. 11 in Ref. [5]). Not realizing this and using the Modified Wheeler Equation at higher breakthrough fractions can lead to errors in analyzing data and calculating breakthrough times or adsorption rate coefficients.

Wood [7] has extended a rearranged Reaction Kinetic Equation (1) to better describe asymmetric (skewed) breakthrough curves with

$$\frac{C}{C_o} = \frac{\exp\{(t - A)/[B + G(t - A)]\}}{\exp\{(t - A)/[B + G(t - A)]\} + [(1 - P_s)/P_s]\exp[-H(t - A)/B]}, \quad (5)$$

where A is the time (t_{sto}) and P_s is the C/C_o ratio for the stoichiometric center of the breakthrough curve. B is

related to A and inversely proportional to the rate coefficient at the stoichiometric center [7]. The two additional parameters, G and H, allow this equation to fit even very skewed breakthrough curves [7]. Eq. (5) has the advantage of reducing to the Reaction Kinetic Equation (1) when G and H are zero; so, it can also describe the ideal case. A disadvantage is that the parameters G and H have not been assigned physical meaning or related to vapor or carbon properties for predictive purposes.

Yoon and Nelson [6] have also published an equation for describing asymmetric cartridge breakthrough curves, particularly those resulting from the presence of high humidity. They assumed that the contaminant saturation capacity, W_e, is a linear function of time: $W_e = W_b(t + W_a)$. Their resulting breakthrough curve equation can be rearranged to give the breakthrough time expression:

$$\frac{C}{C_o} = (1 + \exp[k''\{\ln(W_a + \tau) - \ln(W_a + t_b)\}])^{-1}, \quad (6)$$

where k'', W_a, and τ, the 50% breakthrough time, can be obtained by fitting breakthrough-curve data to Eq. (6) by nonlinear least squares regression. Disadvantages to using Eq. (6) for service life predictions are: (1) some of the fit parameters have no assigned physical meaning, (2) the equation is not defined for $t \leq -W_a$, and (3) the equation does not reduce to the ideal Reaction Kinetic Equation, an equivalent of which the same authors used previously [18].

Assuming the Reaction Kinetic Equation (1) with parameters of the Modified Wheeler Equation (4) and knowing the stoichiometric center time t_{sto} and a breakthrough time (e.g., $t_{10\%}$) at a given breakthrough fraction (e.g., $C/C_o = 10\%$), an experimental rate coefficient (e.g., $k_{v10\%}$) can be calculated as [4]:

$$k_{v10\%}\ (\text{min}^{-1}) = \frac{t_{sto} Q \rho_B [\ln(9)]}{W(t_{sto} - t_{10\%})}. \quad (7)$$

The stoichiometric time [first term of Eqs. (1) and (4)] is a function of the equilibrium adsorption capacity W_e, which can be obtained from adsorption isotherm measurements or calculations without measuring breakthrough curves. Therefore, although t_{sto} is often close to $t_{50\%}$, it is preferable to use t_{sto} derived from integration of the complete breakthrough curve, as

$$t_{sto} = \int_0^\infty (1 - C/C_o)\, dt, \quad (8)$$

or from breakthrough curve fitting to equations such as Eq. (5) [4,7].

We define a skew parameter as $S = k_{v1\%}/k_{v10\%}$. The reasons for this choice are that (1) breakthrough times are most often reported at 1 and 10% breakthrough fractions and (2) ranges of reported breakthrough curves often incorporate the more easily detectable concentrations corresponding to these fractions. Wood [7] observed that rate coefficients (multiplied by constant residence time) determined using the Reaction Kinetic Equation (1) were linear functions of $\log_{10}[(C_o - C)/C]$ for a variety of breakthrough curves and conditions over the range of $C/C_o = 0.1$ to 50% (Fig. A-1 of Ref. [7]), so that

$$k_{v(C/C_o)} = a\left[1 + b \ln\left(\frac{C_o - C}{C}\right)\right]. \quad (9)$$

From the definition of S and for a given breakthrough curve:

$$b = \frac{S - 1}{\ln(99) - S\ln(9)} \quad \text{and} \quad a = \frac{k_{v0.1\%}}{1 + b\ln(999)}. \quad (10)$$

The constant 'a' could also be calculated at any other breakthrough fraction for which a rate coefficient is known. All that remains is obtaining a value or mathematical expression for the skew parameter S.

3. Experimental

At the Los Alamos National Laboratory (LANL) in the 1980s, J.F. Stampfer led a team that measured 305 breakthrough curves for 33 gases and vapors and beds of two types of carbons. Wood and Stampfer [4] reported average 1 and 10% rate coefficients obtained from 165 of these experiments with 27 compounds and one carbon (12–30 mesh ASC Whetlerite). Conditions were: 2 cm bed depth, 2.3 cm bed diameter, 4.55 g carbon, 3% relative humidity, 23 °C, 740 cm/s airflow velocity, and three concentrations (340, 680, and 1320 ppm). Details of the experimental procedure appear in Ref. [4].

Additional breakthrough experiments also included another carbon (12–30 mesh ASZM-3T, an activated carbon impregnated with triethylenediamine and metal salts, but not chromium salts, at 4.78 g/2-cm depth) and six more compounds (acetone, ethyl acetate, chloroform, diethyl ether, perfluorobutane, and perfluoro-2,3-epoxy-2-methylpentane). Test conditions also included 1–6 cm bed depths, 370 cm/s flow velocity, and 3–80% relative humidities (RHs). In nearly all cases, the test beds were preconditioned (PRE) with air flow (usually overnight) at the test (RUN) RH before being used. These conditions will be noted as, for example, PRE RH/RUN RH= 80%RH/80%RH.

We have reanalyzed all 305 breakthrough curves. In order to get 1%, 10%, and stoichiometric breakthrough times by interpolation and extrapolation, we selected only those curves with data including 2 to 80% breakthroughs. Also, since rapidly eluting gases do not have time to form constant pattern wavefronts and there are no practical applications for rapidly eluting gases, we selected only those curves with $t_{1\%} > 2$ min. Five of the C-2 and fluorinated C-2 gases were eliminated. These selections left 191 breakthrough curves for 26 compounds (Table 1)

Table 1
Average adsorption rate coefficients and skew ratios calculated from breakthrough curves at dry conditions (LANL data)

Chemical	Molar polarizability (cm^3/mol)	Adsorption rate coefficient (min^{-1})		Ratio
		$k_{v1\%}$	$k_{v10\%}$	
1,1,1-Trifluoroethane	10.632	2200	1674	1.31
Perfluoropropene	14.483	2268	1755	1.29
1,1,3,3,3-Pentafluoropropene	14.701	2598	2228	1.17
3,3,3-Trifluoropropyne	14.935	2349	1873	1.25
3,3,3-Trifluoropropene	15.137	2533	2141	1.18
Propyne	15.589	2227	1904	1.17
Propene	15.791	2335	1940	1.20
Acetone	16.179	3991	3109	1.28
Perfluoro-2-butyne	17.336	2443	2209	1.11
2-Butyne	18.644	3510	3098	1.13
Perfluorocyclobutene	19.301	2504	1861	1.35
Perfluoro-2-butene	19.912	2917	2490	1.17
Butane	20.632	2916	2153	1.35
Chloroform	21.459	2955	2316	1.28
3,3,4,4,4-Pentafluoro-1-butene	21.575	2910	2590	1.12
2-Butene	21.656	3176	2534	1.25
2-Trifluoromethylpropene	21.863	3393	3072	1.10
Ethyl acetate	22.259	5539	3547	1.56
1,3-Butadiene	22.460	3430	2740	1.25
Isobutene	22.517	3364	3063	1.10
1-Butene	22.665	3532	2989	1.18
3-Methyl-1-butene	24.942	3345	2789	1.20
Diethyl ether	25.693	3296	3354	0.98
Benzene	26.259	4055	3582	1.13
Perfluoro-1-heptene	31.084	3403	2701	1.26
1-Heptene	34.136	4071	3185	1.28
			Average=	1.22
			Standard deviation=	0.11

to be analyzed for skew. We fit each of these remaining breakthrough curves to Eq. (5) using four experimental breakthrough times near 1, 10, 50, and 90% breakthrough fractions. The resulting four parameters A, B, G, and H then allowed interpolation, extrapolation, and integration to get $t_{1\%}$, $t_{10\%}$, and t_{sto}. For each breakthrough curve a rate coefficient $k_{v10\%}$ was then calculated by Eq. (7) and $k_{v1\%}$ by the corresponding one with ln(99).

4. Other databases analyzed

Smoot [19] of the Bendix Corporation (NASA) published a literature review of adsorption equations. This report also included new experimental breakthrough time data for 12 organic liquids and a 12–20 mesh Witco petroleum-based activated carbon (Witcarb 337). Experimental conditions were 1000 ppm vapor concentration, 25 °C, and 32 l/min airflow through a 7-cm-diam. by 2.2-cm-deep bed of packed density 0.40 g/cm^3. Test RHs were 0, 50, and 80%. No preconditioning was mentioned, but similar listed values of starting carbon weights at each RH and listed water uptakes at the higher RHs imply that all the carbon samples were dry to start with (noted as Dry/RUN %RH).

Smoot reported at least duplicate experiments at each RH for each compound. We analyzed 121 of the individual breakthrough experiments for which 1, 10, 50, and 90% breakthrough times were all reported. We fit each of these breakthrough curves to Eq. (5) to get the stoichiometric time for calculating $k_{v10\%}$ by Eq. (7) and $k_{v1\%}$ by the corresponding equation for 1% breakthrough.

In the 1970s, Nelson and coworkers measured 618 vapor breakthrough curves for 121 chemicals and three types of activated carbons in commercial respirator cartridges at the Lawrence Livermore National Laboratory (LLNL). Test conditions, results, analyses, and conclusions from these were reported in a series of papers culminating in a summary in Ref. [5]. Other variables included vapor concentration, airflow rate, number of cartridges (one or two) in parallel, preconditioning RH, and test RH. Nelson [20] has provided us with the original full experimental breakthrough curve data, test conditions, final water loadings, interpolations of 1 and 10% breakthrough times, and calculated curve geometric centroids (stoichiometric times and fractions) for the 618 curves. With this data we again

calculated $k_{v1\%}$ and $k_{v10\%}$ for each curve by equations such as Eq. (7).

5. Results and discussion

5.1. LANL results

Table 1 lists 26 gases and vapors and averages (for all concentrations and replicates meeting the breakthrough curve criteria discussed previously) of 1 and 10% rate coefficients calculated for each breakthrough curve. The table also shows ratios of these averages. These results are for only the driest (3% RH/3% RH) test conditions and a single carbon [4]. Chemicals are listed in order of increasing polarizability and, therefore, carbon affinity [3]. The overall average of these average ratios was 1.22 with a standard deviation of 0.11. There is no trend of the ratios with increasing polarizability and affinity, although there is a general trend of increasing rate coefficients, as expected [2,4]. From these results we conclude that the average ratio (skew parameter S) is statistically greater than 1.00 and that breakthrough curve skew for these conditions is independent of the chemical type.

Fig. 2 shows a plot of $k_{v1\%}$ vs. $k_{v10\%}$ for all PRE RHs/RUN RHs and both carbons from the LANL study. Except for the 3% RH/3% RH averages taken from Table 1, plotted points are calculated from individual breakthrough curves. The reference line has a slope of 1.5. The $k_{v1\%}/k_{v10\%}$ ratios (skew parameters, slopes from the origin to plotted points) are highest for the lowest rate coefficients, which correspond to the highest RHs. The two carbons and 26 chemicals are in good agreement with one another. This graph raises the question as to whether the decrease in skew at a higher rate coefficient is due to lower RH or to the higher rate coefficient.

5.2. NASA results

Fig. 3 shows the same kind of plot for the 121 NASA breakthrough curves. We consider the open symbols (all nine ethyl acetate data and one carbon tetrachloride test out of seven replicates) as significant outliers for unknown reasons and do not include them in further analyses. The remaining 111 data for dry carbon beds and 0, 50, and 80% RUN RH all seem to fall on a common straight line with an average slope of 1.27 (0.13 standard deviation).

This slope for the unimpregnated carbon is close to the 1.22 average ratio obtained for two impregnated carbons and dry conditions in the LANL study (Table 1). Again, there is no effect of chemical type on the slope. However, unlike the LANL results, there is apparently no effect of RUN RH on slope or rate coefficient magnitude. We attribute this difference to lack of RH preconditioning in the NASA study. This lack of RUN RH effect is consistent with the essentially identical calculated micropore volumes and adsorption energies reported in the NASA report [19] at all three RUN RHs.

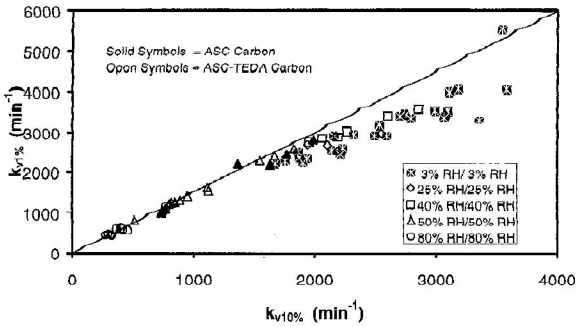

Fig. 2. A comparison of 1 and 10% breakthrough rate coefficients for two activated carbons and five relative humidity conditions (LANL data). The reference line represents a slope (rate coefficient ratio) of 1.5.

5.3. LLNL results

To answer the question raised in the LANL study, Fig. 4 is a plot of rate coefficients from 458 Dry/Dry (Dry~ RH≤50%) LLNL breakthrough curves. The reference straight line in Fig. 4 has a slope of 1.00 (no skew). This dry condition data fit a curve and a quadratic equation (listed on Fig. 4) better than a straight line, which suggests that the curvatures here and in Fig. 2 cannot be attributed to differing humidity conditions. When the higher RH data from the LLNL studies are included, the graph with 618 points looks very much like Fig. 4 and has a quadratic equation fit of $y = 1.40x - 0.0000338x^2$.

Fig. 5 shows LLNL skew parameters averaged for a variety of chemicals as functions of RUN RH and PRE RHs. Within ±0.05 the average ratios are constant and

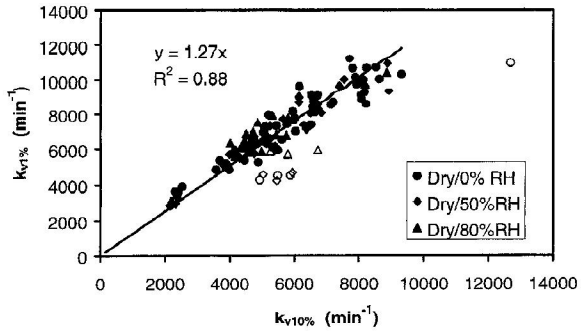

Fig. 3. A comparison of 1 and 10% breakthrough rate coefficients for dry carbon beds run at three relative humidities (NASA data). The open symbols represent nine ethyl acetate and one carbon tetrachloride data treated as outliers. The line and equation are from a linear least squares fit through the origin without the outliers.

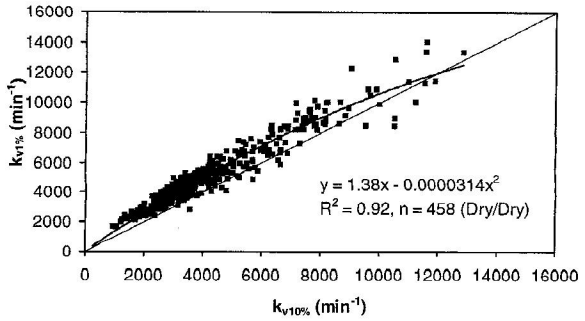

Fig. 4. A comparison of 1 and 10% breakthrough rate coefficients for dry carbon beds run at dry conditions (LLNL data).

similar to the LANL and NASA averages of 1.22 and 1.27, respectively, until RUN RH and PRE RH both exceed 50%. For reasonably dry beds (PRE RH $\leq$50%), there is no change in S up to and including 80% RUN RH. This conclusion is in agreement with the NASA results. At >50% RUN RH and PRE RH, the ratio increases.

An analysis of the effect of final (at the end of each experiment and complete breakthrough) water loading (Fig. 6) shows that S increases with water loading to a maximum at 1.4. The question remains as to whether water loading increases skew directly or indirectly by reducing the magnitude of the adsorption rate coefficient [21]. Water apparently does not block the most active adsorption sites that are responsible for skew.

5.4. All results

The 793 data (excluding outliers mentioned) from these three studies at all RH conditions and for all carbons are plotted together in Fig. 7. The quadratic equation shown on the graph is equivalent to the following expression for the skew parameter defined above:

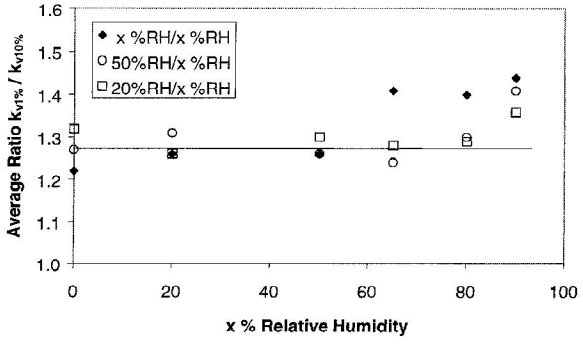

Fig. 5. Effect of preconditioning and test relative humidities (PRE RH/RUN RH) on average skew parameters (LLNL data).

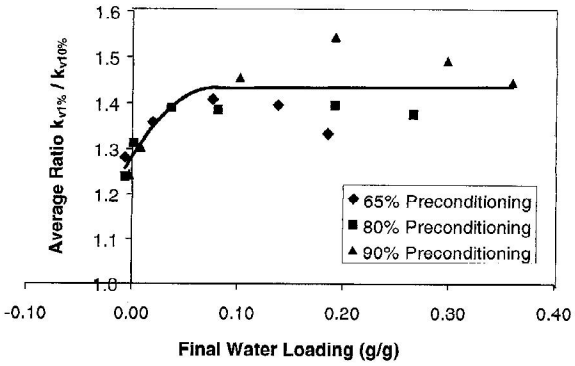

Fig. 6. Effect of water loading at the end of complete breakthrough on skew parameters averaged for all compounds at each test relative humidity, which ranged from 20 to 90% (LLNL data).

$$S = 1.41 - 0.0000324k_{v10\%}. \quad (11)$$

The standard deviation of the 793 data from this equation is 0.11. The limit of S at high rate coefficients seems to be 1.00 (no skew).

6. Application and conclusions

As stated in the Introduction, one application of the above skew analysis is to estimate an adsorption rate coefficient at a desired breakthrough fraction from one known at another breakthrough fraction. Eq. (9) can be used to generalize Eq. (11) as:

$$S = 1.41 - 0.0000324\left[\frac{1 + b\ln(9)}{1 + b\ln([C_o - C]/C)}\right]k_{v(C/C_o)}, \quad (12)$$

with an upper limit of $S \leq 1$. We can then apply the definition of S to get:

$$S = \left[\frac{1 + b\ln(99)}{1 + b\ln(9)}\right]. \quad (13)$$

Eqs. (12) and (13) can be solved for 'b' using the quadratic root equation:

$$b = \frac{-B - \sqrt{B^2 - 4AC}}{2A}, \quad (14)$$

where for known $\ln(r) = \ln([C_o - C]/C)$ and $k = k_{v(C/C_o)}$, then $A = -1.497\ln(r) - 0.0001564k$, $B = 0.41\ln(r) - 0.0001423k - 1.497$, and $C = 0.41 - 0.0000324k$. Also, $a = k/[1 + b\ln(r)]$.

For example, Lodewyckx and Vansant [21] reported an experimental Wheeler–Jonas Equation (4) rate coefficient $k_{v0.1\%} = 5763$ min^{-1} for carbon tetrachloride at Dry/Dry conditions with a BPL-HA carbon. Solving Eq. (14) we

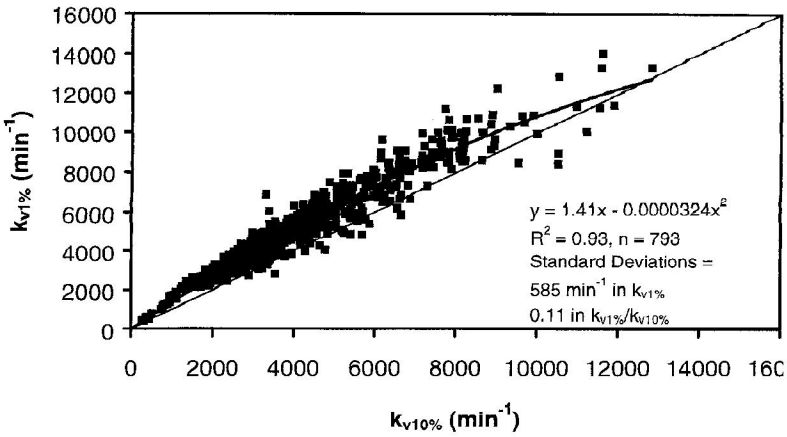

Fig. 7. A comparison and correlation of 1 and 10% breakthrough rate coefficients for all carbon beds, chemicals, and test conditions (LANL, NASA, and LLNL databases).

get $b = 0.166$ and $a = 2685$, so that at 1% breakthrough $k_{v1\%} = 4733$ min^{-1} by Eq. (9) and $S = 1.29$ from the definition of S. Since ln(1000) = 6.908 in the Wheeler–Jonas Equation (4) is very close to ln(999) = 6.907 in the Reaction Kinetic Equation (1), the reference rate coefficient for the former can be used for the latter. However, at higher (>0.032) breakthrough fractions this assumption is less appropriate and corrections must be made using ratios of the log terms [e.g., ln(9)/ln(10) for 10% breakthrough].

An advantage of this approach to quantifying skew is that the simple, ideal Reaction Kinetic Equation can still be used, even for nonideal, asymmetric breakthrough curves. The correlations developed above were not based on and do not apply to rapidly eluting ($t_{1\%} < 2$ min) gases, whose breakthrough curves, however, we have observed to be even more skewed (slightly later breakthrough times at lowest breakthrough fractions) than predicted by the above correlations.

References

[1] Wood GO. Estimating service lives of organic vapor cartridges. Am Ind Hyg Assoc J 1994;55:11–5.
[2] Lodewyckx P, Vansant EF. Estimating the overall mass transfer coefficient k_v of the Wheeler–Jonas equation: a new and simple model. Am Ind Hyg Assoc J 2000;61:501–5.
[3] Wood GO. Activated carbon adsorption capacities for vapors. Carbon 1992;30:593–605.
[4] Wood GO, Stampfer JF. Adsorption rate coefficients for gases and vapors on activated carbons. Carbon 1993;31:195–200.
[5] Nelson GO, Correia AN. Respirator cartridge efficiency studies: VIII. Summary and conclusions. Am Ind Hyg Assoc J 1976;37:514–25.
[6] Yoon YH, Nelson JH. A theoretical study of the effect of humidity on respirator cartridge service life. Am Ind Hyg Assoc J 1988;49:325–33.
[7] Wood GO. Organic vapor respirator cartridge breakthrough curve analysis. J Int Soc Resp Prot 1993;10(4):5–17.
[8] Lavanchy A, Stoeckli F. Dynamic adsorption of vapour mixtures in active carbon beds described by the Myers–Prausnitz and Dubinin theories. Carbon 1997;35:1573–9.
[9] Bohart GS, Adams EQ. Some aspects of the behavior of charcoal with respect to chlorine. J Am Chem Soc 1920;42:523–44.
[10] Danby CJ, Davoud JG, Everett DH, Hinshelwood CN, Lodge RM. The kinetics of adsorption of gases from air stream by granular reagents. J Chem Soc 1946;:918–34.
[11] Yoon YH, Nelson JH. Application of gas adsorption kinetics I. A theoretical model for respirator cartridge service life. Am Ind Hyg Assoc J 1984;45:509–15.
[12] Vermeulen T, LeVan MD, Hiester NK, Klein G. Adsorption and ion exchange. In: Perry RH et al., editor, Perry's chemical engineers handbook, 6th ed., New York: McGraw-Hill, 1984, pp. 1–48, Section 16.
[13] Mecklenburg W. Uber schichtenfiltration, ein beitrag zur theorie der gasmaske. Z Electrochem 1925;31:488–95; Mecklenburg W. Uber schichtenfiltration, ein beitrag zur theorie der gasmaske. Kolloid Zh 1930;52:88–103.
[14] Klotz M. The adsorption wave. Chem Rev 1946;39:241–68.
[15] Gamson BW, Thodos G, Hougen OA. Heat, mass and momentum transfer in the flow of gases through granular solids. Trans Am Inst Chem Eng 1943;39:1–35.
[16] Wheeler A, Robell AJ. Performance of fixed-bed catalytic reactors with poison in the feed. J Catal 1969;13:299–305.
[17] Jonas LA, Rehrmann JA. The kinetics of adsorption of organo-phosphorus vapors from air mixtures by activated carbons. Carbon 1972;10:657–63.
[18] Yoon YH, Nelson JH. Application of gas adsorption kinetics II. A theoretical model for respirator cartridge service life and its practical applications. Am Ind Hyg Assoc J 1984;45:517–24.

[19] Smoot DM. Development of improved respirator cartridge and canister test methods. The Bendix Corporation, NASA Launch Support Division, Cocoa Beach, FL. Unpublished report for U.S. Department of Health, Education, and Welfare, contract NAS10-8842, 1977.

[20] Nelson GO. Miller-Nelson Research Inc., Monterey, CA. Private communication, 1988.

[21] Lodewyckx P, Vansant EF. The influence of humidity on the overall mass transfer coefficient of the Wheeler–Jonas equation. Am Ind Hyg Assoc J 2000;61:461–8.